J. Chil. Chem. Soc., 63, Nº 3 (2018)

THERMAL STABILITY OF THE Cu-CeO_2 INTERFACE ON SILICA AND ALUMINA, AND ITS RELATION WITH ACTIVITY IN THE OXIDATION REACTION OF CO AND THE DECOMPOSITION OF N_2O

*PABLO ALVAREZ[(1)], GONZALO AGUILA[(2)], SICHEM GUERRERO[(3)] AND PAULO ARAYA[(1)]**

[(1)]Departamento de Ingeniería Química, Biotecnología y Materiales, Facultad de Ciencias Físicas y Matemáticas, Universidad de Chile, Beauchef 851, Santiago, Chile.
[(2)]Departamento de Ciencias de la Ingeniería, Facultad de Ingeniería, Universidad Andres Bello, Antonio Varas 880, Providencia, Santiago, Chile.
[(3)]Facultad de Ingeniería y Ciencias Aplicadas, Universidad de los Andes, Monseñor Álvaro del Portillo 12455, Las Condes, Santiago, Chile.

ABSTRACT

The effect of the support on the formation of the Cu-CeO_2 interface and its thermal stability after calcination at 500, 700 and 900 ºC is studied. The supports used are SiO_2, because of its inert character, and Al_2O_3, because it can interact with the Cu and Ce species on the surface. The catalysts were characterized by BET, XRD, UV-vis DRS, and TPR with H_2. The catalytic activity in the CO oxidation reactions with O_2 at low temperature and the decomposition of N_2O were selected to visualize the effect of temperature on the concentration of Cu-CeO_2 interfacial sites. The results show that at a calcination temperature of 500 ºC the formation of the Cu-CeO_2 interface is favored over the SiO_2 support. However, the stability of the Cu-CeO_2 interface on SiO_2 is much lower than on Al_2O_3, causing a substantial decrease of the interfacial sites calcining at 700 ºC, and segregation of the Cu and Ce species on the surface of the silica, with complete loss of the catalytic activity in both reactions when calcining at 900 ºC. In contrast, on alumina the Cu-CeO_2 interface is more stable and presents a significant catalytic activity in both reactions, even when calcining at 900 ºC. The characterization results show that the sintering process of Cu species and CeO_2 particles is less on the alumina support due to the greater interaction of the Cu and Ce with this support.

KEYWORDS: Cu, Ce, silica, alumina, CO oxidation, N_2O decomposition.

1.- INTRODUCTION

The CuO-CeO_2 system has shown excellent catalytic properties for a series of reactions including the oxidation of CO with O_2 [1, 2] and the WGS reaction between CO and H_2O, which produces H_2 and CO_2 [3]. Furthermore, in the oxidation of CO with O_2, the Cu-CeO_2 system has proven to be even more active than Pt supported catalysts [4]. The CuO-CeO_2 system is also very active and selective in its preferential oxidation of CO with O_2 in the presence of H_2 (PROX reaction), making it a very attractive system to generate H_2 with the high purity required by fuel cells [5].

In both reactions, the CO oxidation and the WGS, the Cu-CeO_2 interface sites play an important role in the activity of the catalyst. The facility of the Ce (III) - Ce (IV) redox cycle and the high mobility of oxygen in the crystal structure of CeO_2 are two important properties of CeO_2 [6]. As a result, this oxide is capable of reversibly "adsorbing" oxygen. The high activity of the CuO-CeO_2 system as part of the CO oxidation with O_2 is attributed to the strong interaction between the Cu particles and the CeO_2 phase. Martinez-Arias et al. [7] proposed that CO reacts with oxygen in the Cu-CeO_2 interface, even at room temperature to produce CO_2 resulting in Cu^{1+} and Ce^{3+} formation and leaving an oxygen vacancy in the interface. Another molecule of CO can be adsorbed on the Cu^{1+}, which accounts for the observation of this species by IR during the reaction. Re-oxidation of the surface occurs by the adsorption of O_2 from the gas phase in a mechanism of the Mars Van Krevelen type. The limiting reaction step should be some of the stages of re-oxidation of the catalyst (migration and/or dissociation of oxygen). The controversy on the exact nature of the active sites, the oxidation state of copper, and the reaction mechanism continues [8-11], but what is clear is that the sites are located on the interface between Cu and Ce. Regarding the WGS reaction, the generation of oxygen vacancies in the interface has often been cited as the reason for the high activity of this system. Indeed, in the redox mechanism used to explain this reaction, it is proposed that the H_2O molecule adsorbs on an oxygen vacancy, where the abstraction of oxygen and the generation of H_2 takes place. Subsequently, the oxygen atom is removed by CO which is adsorbed on a neighboring Cu site in the interface, generating a new oxygen vacancy on the surface and allowing the catalytic cycle to continue [3,12].

It was recently reported that the CuO-CeO_2 system is also a highly active component in the direct decomposition of N_2O into N_2 and O_2 [13-16]. This system generates a complete N_2O decomposition in a stream of 2500 ppm of N_2O at temperatures below 550 °C [16]. The abatement of N_2O is very important in controlling greenhouse gases, since it is known that, besides being a toxic gas, N_2O contributes heavily to the greenhouse effect [16]. One of the main sources of N_2O is the industrial production of nitric acid by ammonia oxidation [13]. There are different options for abating N_2O depending on where the catalytic process is performed. It has been found that the best choices for existing plants, are locating the catalyst just under the Pt metal gauze in the ammonia burner (process-gas option), or in the tail-gas train (tail-gas option) [13]. In the first option, the catalyst must be able to withstand high temperatures, near 850 °C, while in the latter, conditions and temperatures are more moderate and the catalyst must work at temperatures near 500 °C. Some commercial catalysts for N_2O process-gas decomposition are: CuO/Al_2O_3 (BASF), $La_{0.8}Ce_{0.2}CoO_3$ (Johnson Matthey), Co_2AlO_4/CeO_2 (Yara International), and $Fe\text{-}Al_2O_3$ (PKR2-INS). Furthermore, Uhde EnviNOx® markets a tail-gas process for removing N_2O and NOx that uses iron-containing zeolites.

Considering the moderate temperature range that was studied in the CuO -CeO_2 system (ambient to 700 °C) [15, 16, 13], in principle, these catalysts could be used in a tail-gas process. The high activity of the CuO-CeO_2 system in N_2O decomposition was attributed to the existence of oxygen vacancies in the interface of the Cu-Ce sites that stabilize Cu^+, which is responsible for the abstraction of the oxygen atom from the N_2O molecule [14].

As shown in all these reactions, as well as other reactions catalysed by the CuO-CeO_2 system, the formation of the Cu-CeO_2 interface is essential for obtaining a catalytically active system. In many cases, the Cu-CeO_2 system is formed either by co-precipitating the precursors of both metals or by using a method that leads to the formation of mixed oxides [14, 15] or by supporting Cu on previously formed CeO_2 [15, 16]. Indeed, all reports that discuss the activity of the CuO-CeO_2 system in decomposing N_2O [13-16], use Cu catalysts that are supported on CeO_2 or use mixed oxides prepared by coprecipitation. A disadvantage to these catalysts is that they are produced with specific areas below 100 m^2/g [18], and most often, even areas of less than 50 m^2/g [19, 20], unless special methods of preparation are used, such as a reversed micro emulsion method [8] in which the mixed oxide reaches areas between 130 and 150 m^2/g after calcination at 500 °C. Furthermore, the specific surface area of these catalysts decreases strongly with increasing calcination temperature. Djinovic at al. [21] show that the specific surface area of a CuO/CeO_2 catalyst decreases from 40.2 m^2/g (at 450 ° C), to only 8.3 m^2/g after calcining at 550 °C. With the goal of improving the thermal stability of CeO_2, the addition of some dopants such as ZrO_2 or La_2O_3 to the cerium oxide has been explored [22, 23]. Alternatively, the CuO-CeO_2 system could be supported on a third oxide with high specific surface area and high thermal stability, with the added advantage that the catalyst acquires the mechanical properties of the support [24]. Regardless of the reason for using a third oxide for support, it is important for the Cu and CeO_2 to interact on the support's surface forming a Cu-CeO_2 interface with a high interfacial area.

In our laboratory, in recent years we have conducted a series of studies using monometallic CuO catalysts and bimetallic CuO-CeO_2 catalysts supported on different oxides that are commonly used as supports: SiO_2, Al_2O_3, and ZrO_2 [25]. Reactions in which these catalysts have been tested include the CO oxidation with O_2 and the WGS reaction.

e-mail: arayap@ing.uchile.cl

In the oxidation reaction of CO with O_2 on a Cu supported monometallic catalyst, the support plays an important role in the activity of the catalysts as shown by the significantly greater activity generated by zirconium oxide catalysts compared to that seen with SiO_2 and Al_2O_3 supports [25]. Regardless of the support used, the addition of CeO_2 generates bimetallic catalysts that are much more active than the monometallic ones. This increase in activity is due to the formation of the Cu-CeO_2 interface on the support's surface, as indicated by various catalyst characterization techniques [25, 26]. However, the formation of the Cu-CeO_2 interface does not occur in the same way on all supports. In fact, when using SiO_2 as support, Cu-CeO_2 generates a more active interface, while the Al_2O_3 support generates a less active interface. This was attributed to the inert character of the silica, which promotes the formation of an interface similar to that formed by supporting Cu directly on CeO_2.

While the inert character of the silica seems to be favorable for the formation of a Cu-CeO_2 interface that is highly active in the oxidation of CO with O_2 and in the WGS reactions, inertness can generate a problem with the stability of this interface at high temperatures. Indeed, if a catalyst with 2% Cu and 8% Ce, prepared by coimpregnation of the nitrates of both metals on SiO_2 (Aerosil 200), is calcined at 500 °C, a highly active catalyst for CO oxidation is obtained which has a practically 100% conversion rate below 140 °C. However, if the calcination temperature is increased to 650 °C or higher temperatures, a marked decrease in catalytic activity occurs, falling to practically 0 when calcining at 700 °C [26]. The characterization of the catalysts calcined at different temperatures show that the Cu-CeO_2 interface practically disappears due to calcination at 700 °C, accounting for its sharp drop in activity. It is reasonable to assume that the inert character of SiO_2 facilitates both the migration and sintering of Cu and Ce species, reducing the Cu-CeO_2 interface sites on the carrier's surface.

Since it is known that Cu can interact with the Al_2O_3 support [27, 28], especially at low loads, it is also reasonable to assume that the thermal stability of the Cu-CeO_2 interface formed on this oxide can be greater than that formed on the essentially inert SiO_2 surface. This is the hypothesis that gives rise to the present paper, where the effect of the supports, SiO_2 and Al_2O_3, on the topography of the Cu-CeO_2 interface and on its stability under calcination between 500 ºC and 900 ºC is compared. The activity of the catalysts in the CO oxidation and N_2O decomposition reactions are used as test reactions, because both reactions are highly dependent on the existence of the Cu-CeO_2 interface.

Although the oxidation reactions of CO can occur at temperatures considered moderate, below 300 °C, in other reactions such as the process-gas option for decomposing N_2O, the temperature can be in the range of 850 to 900 °C, justifying the study of the stability of the Cu-CeO_2 interface at high temperatures.

2.- EXPERIMENTAL

2.1 Catalyst Preparation

The catalysts were prepared by coimpregnation of the support with a solution containing Cu and Ce nitrates, with a total loading of 2% Cu and 8% Ce. They were then dried at 105 °C overnight and calcined at the required temperature, 500 ºC, 700 ºC, and 900 ºC. The supports used were commercial SiO_2 (Aerosil 130) and γ-Al_2O_3 (Sigma-Aldrich). The catalysts will be denoted as Cu/X-Y and CuCe/X-Y, where X is the support silica (Si) or alumina (Al), and Y is the catalysts calcination temperature (500, 700 or 900).

2.2 Catalyst Characterization

The samples were characterized by N_2 adsorption, X-ray diffraction (XRD), temperature-programmed reduction in a hydrogen stream (TPR), and UV-vis DRS.

The determination of the specific surface area of the catalysts was made by measuring N_2 adsorption in a model ASAP 2010 Micromeritics sorptometer. The samples were previously degassed at 200 ºC.

The crystal structure of the different catalysts was determined on a Siemens D-5000 diffractometer using Cu Kα radiation and a scan rate of 0.02 degrees per minute.

The temperature-programmed reduction analyses were made on a conventional system equipped with a TCD detector, with a flow of 20 cm^3/min of a gaseous mixture of 5% H_2 in Ar, and a heating ramp of 10 °C/min between ambient temperature and 700 ºC.

Finally, the UV-vis DRS analyses were made on a Perkin Elmer Lambda 650 instrument equipped with a Harrick Praying Mantis and powder cell.

2.3 Measurement of Catalyst Activity

CO oxidation*:* The kinetics tests were made in a piston flow tubular reactor, with 2% CO and 3% O_2 streams at a total flow rate of 100 cm^3/minutes. After loading the reactor with 0.1 g of catalyst, the sample was pretreated at 300 ºC for one hour in O_2, and the reactor was cooled to room temperature. The reactants were then fed and the temperature was increased at a rate of 3 ºC/min, taking samples every 20 ºC to determine the concentration of CO, O_2, and CO_2 on a Perkin Elmer Autosystem chromatograph with a CTR column (Alltech) and a TCD detector.

N_2O decomposition*:* The catalytic activity tests were also performed in a piston flow tubular reactor, with a flow of 5000 ppm N_2O balanced in He, at a total flow rate of 100 cm^3/min, operated at atmospheric pressure. After loading the reactor with 0.35 g of catalyst, the catalyst was pretreated at 400 ºC with O_2 for 30 min and then at 600 ºC for 1 h with He. After the pretreatment, the reactor temperature was decreased to 350 ºC, and the reactant (N_2O balanced in He) was then fed to the reactor. After 30 min of N_2O flow, the temperature was increased from 400 ºC to 600 ºC, taking samples every 25 ºC to determine the concentration of N_2O on a Perkin Elmer Autosystem chromatograph equipped with a HAYASEP D column and a TCD detector.

3.- RESULTS

3.1 Characterization of the catalysts

Table 1 shows the BET area of the different mono- and bimetallic catalysts. In the case of the SiO_2 support, increasing the calcination temperature from 500 to 900 ºC has little effect on the specific surface area of the catalysts, as expected from the high thermal stability of silica. In the case of the monometallic Cu catalysts, the specific surface area decreases from 130 to 110 m^2/g when calcining between 500 and 900 ºC, while in the bimetallic Cu-Ce catalysts the specific surface area decreases from 128 to 104 m^2/g over the same calcination temperature range.

In the case of the Al_2O_3 support, in the monometallic Cu as well as in the bimetallic Cu-Ce catalysts, increasing the calcination temperature of the catalyst has some effect on the specific surface area between 500 ºC and 700 ºC. In the case of the monometallic catalysts, the area varies between 130 and 111 m^2/g when calcining between 500 and 700 ºC, while with the bimetallic catalysts the area decreases from 109 to 96 m^2/g for the same temperature range. However, with calcining at 900 ºC, the specific surface area of the mono- and bimetallic catalysts decreases to around 60 m^2/g, showing the lower thermal stability of alumina.

Table 1. BET specific surface area and H_2 consumption of the various monometallic and bimetallic catalysts.

Catalyst	BET Surface Area (m^2/g)	Ratio of: H_2 consumed / H_2 required for complete reduction of CuO	CeO_2 particle diameter (nm)
Monometallic			
Cu/Si-500	130	0.99	-
Cu/Si-700	120	1.01	-
Cu/Si-900	110	1.02	-
Cu/Al-500	130	0.82	-
Cu/Al-700	111	0.60	-
Cu/Al-900	60	0.59	-
Bimetallic			
CuCe/Si-500	128	1.33	6.0
CuCe/Si-700	128	1.08	6.8
CuCe/Si-900	104	0.99	12.0
CuCe/Al-500	109	1.04	5.7
CuCe/Al-700	96	0.69	6.3
CuCe/Al-900	58	0.64	7.1

The effect of the calcination temperature on the crystal structure of

the catalysts supported on SiO_2 is shown in Figure 1A. In the case of the monometallic catalysts, the peaks of the tenorite structure of CuO at 2θ = 35.5º and 38.7º are seen clearly in all the catalysts calcined between 500 ºC and 900 ºC: Cu/Si-500, Cu/Si-700 and Cu/Si-900. These results confirm what has been reported previously [25, 26], and show that Cu forms crystalline CuO particles on silica, even at low calcination temperatures (500 ºC). In contrast, in the diffractograms of the bimetallic Cu-Ce catalysts, the CuO peaks are no longer seen in the catalysts calcined at 500 ºC (CuCe/Si-500) and 700 ºC (CuCe/Si-700), and they can only be seen weakly in the bimetallic catalyst calcined at 900 ºC (CuCe/Si-900). The effect of the increased dispersion of Cu by adding CeO_2 has been reported in the literature [25, 26, 29], so it is not strange for the CuO peaks to disappear in the bimetallic catalysts calcined at 500 ºC and 700 ºC.

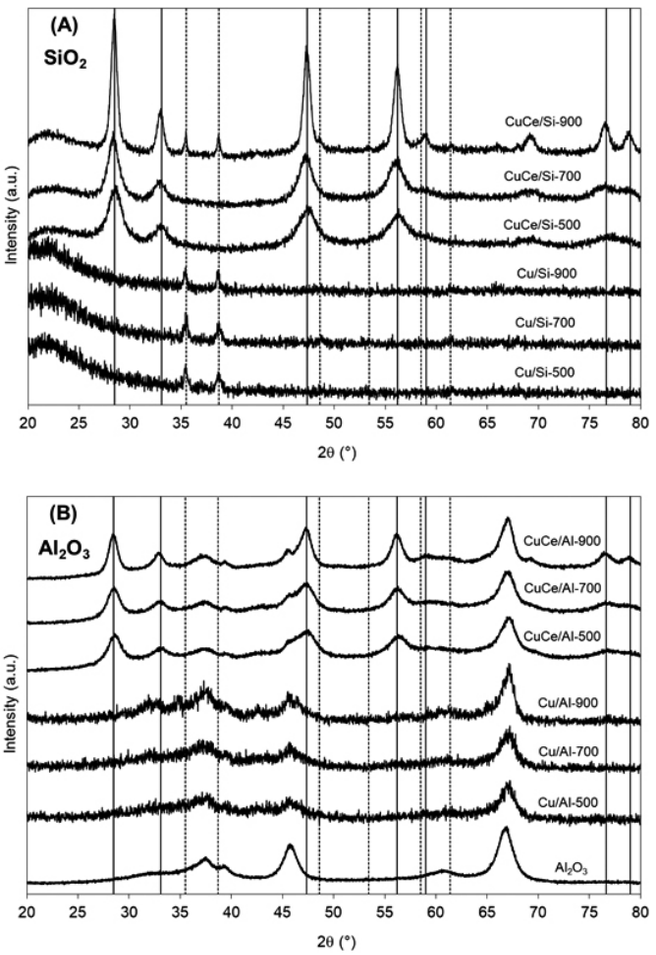

Figure 1: XRD patterns of monometallic (Cu) and bimetallic (CuCe) catalysts calcined at 500 °C, 700 °C and 900 °C. (A) Supported on SiO_2; (B) Supported on Al_2O_3. The diffraction lines of CuO (·····) and CeO_2 (——) are indicated as reference. Operation conditions: scan range = 20 - 80 °; scan rate = 0.02 degrees per minute.

The appearance of the CuO peak at 900 ºC is, therefore, a clear indication of substantial segregation of CuO and CeO_2 on the silica surface of CuCe/Si-900 catalyst. In all the bimetallic catalysts the peaks at 2θ = 28.6º, 33.1º, 47.5º, and 56.4º, attributable to the fluorite structure of cerium oxide, are clearly seen. In the case of the catalyst calcined at 900 ºC, the peaks of CeO_2 at 2θ = 59.0º, 76.7º, and 79.2º are also visible. The particle size of CeO_2 calculated by means of Scherrer's equation is also given in Table 1. As expected, the temperature increase leads to a strong growth of the CeO_2 particle size, from 6.0 nm after calcination at 500 ºC, to 12.0 nm after calcination at 900 ºC.

Figure 1B shows the diffractograms of catalysts supported on alumina. The diffractograms of all the catalysts are dominated by the peaks corresponding to γ-alumina. Those located at 2θ = 37.6, 39.5, 45.8, 60.5, and 66.8º are the most intense. Regardless of the calcination temperature, the peaks corresponding to CuO or crystalline $CuAl_2O_4$ are not found in any of the catalysts. The classic studies of Friedman et al. [27] and Stromehier et al. [28] show that at low loads the Cu enters the defect spinel of the γ-alumina support to yield a well dispersed phase which is not detected by X-ray diffraction [27,28]. This Cu structure is usually cited as "copper aluminate surface phase" because it "resembles" the $CuAl_2O_4$ phase. According to these authors, as long as the Cu load does not exceed 4%-5% for every 100 m^2/g, the appearance of CuO is not expected [27, 28]. Considering the above, it is not strange that in our catalysts the formation of crystalline CuO is not seen. On the other hand, the formation of Cu aluminate can be observed by XRD at greater Cu loads and higher calcination temperatures. In fact, Luo et al. [30] report the formation of Cu aluminate in catalysts with 11% or higher loads at temperatures above 800 ºC. Because of this, no copper aluminate is expected in our catalysts. In the case of the bimetallic Cu-Ce catalysts, CeO_2 peaks are seen at 2θ = 28.6, 33.1, 47.6, and 56.4º. As reported in Table 1, although the size of the CeO_2 crystal increases from 5.7 nm at 500 ºC to 7.1 nm at 900 ºC, this increase is noticeably less than that observed in the catalysts supported on silica. It is clear, therefore, that the greater interaction of the CeO_2 particles with alumina decreases the degree of sintering with the temperature increase. The peaks corresponding to crystalline CuO are not detected by XRD in any of the catalysts, regardless of the calcination temperature, for the reasons already discussed for the monometallic catalysts supported on alumina.

The results of the temperature programmed reduction (TPR) experiments using H_2 as reductant are shown in Figure 2A for silica supported catalysts, and Figure 2B for alumina supported catalysts.

In the case of the monometallic catalysts supported on SiO_2, there is only one reduction peak, with a maximum that is displaced from 290 ºC to 308 ºC by calcining between 500 and 900 ºC (Figure 2A). This peak has been seen in previous work by our group [25], and, according to the literature, it can be associated with bulk CuO [31-33]. The assignment of this peak to bulk CuO agrees with what has been observed in the XRD diffractograms, which show clearly the formation of crystalline CuO in all the monometallic Cu catalysts supported on silica. Table 1 reports the consumption of H_2 by the different catalysts, expressed as the ratio between the consumed H_2 and the H_2 required to reduce all the Cu^{2+} to Cu^0. All the fractions are very close to 1.0, indicating that the reduction of the Cu oxide to metallic Cu is complete in the temperature range used in the TPR experiments.

In the case of the bimetallic catalysts, with the catalysts calcined at 500 ºC (CuCe/Si-500), the reduction occurs at a considerably lower temperature than with the monometallic catalysts. In effect, two reduction peaks are seen with maxima at 195 and 214 ºC. The appearance of two reduction peaks agrees with what was seen in previous work [25, 26]. According to the literature the first peak is associated with the reduction of highly dispersed Cu species in contact with CeO_2, and the second peak with the reduction of Cu particles (clusters), but also in contact with CeO_2. On the other hand, as shown in Table 1, the ratio of the consumption of H_2 is greater than 1, indicating that another species is being reduced together with Cu species. The literature reports that CeO_2 is reduced above 380 ºC, but when Cu interacts with the CeO_2 particles part of the CeO_2 is reduced together with the Cu [4, 25, 34], therefore accounting for a ratio greater than 1. Therefore, the result shown in Table 1 (ratio = 1.33) confirms the idea that the Cu species are interacting strongly with CeO_2 in the catalysts calcined at 500 ºC. As the calcination temperature is increased to 700 ºC, only one maximum is seen around 265 ºC, which can be associated with larger Cu particles interacting with CeO_2. At the same time, the overconsumption of H_2 reported in Table 1 decreases strongly in this catalyst (ratio = 1.08), suggesting that the interaction between Cu and CeO_2 also decreases by calcining at 700 ºC. Finally, calcining at 900 ºC a single peak is seen with a maximum at 308 ºC, which can be assigned to the reduction of bulk CuO particles that do not interact with CeO_2. In fact, this peak is located at practically the same temperature as the one seen in the monometallic catalyst. Again, this assignment agrees with the XRD results, which show the formation of crystalline CuO when calcining the bimetallic catalyst at 900 ºC. Furthermore, the results of the consumption of H_2 shown in Table 1 (ratio = 0.99) indicates that in this catalyst there is practically no overconsumption of H_2, and therefore the only species that is reduced is CuO, reflecting the separation of the CuO and CeO_2 particles on the surface of the SiO_2 support when calcining at 900 °C.

The H_2 consumption curves (TPR) of catalysts supported on alumina are shown in Figure 2B. In the case of monometallic catalyst calcined at 500 ºC (Cu/Al-500), there is a main reduction peak with a maximum at 280 ºC. The literature is somewhat contradictory in assigning this reduction peak. At low Cu loads, Dow et al. [35] report a single reduction peak associated with highly dispersed Cu at about 210 ºC, while the formation of bulk CuO occurs only at

Cu loads greater than 5%, generating a second peak with a maximum close to 245 ºC. Yao et al. [36] also saw one reduction peak at low Cu loads, but with a maximum at 300 ºC which they attributed to highly dispersed Cu, forming isolated and two- and three-dimensional small copper clusters. Xiaoyuan et al. [37] also found a single reduction peak with a maximum at 317 ºC for a 1% Cu on alumina catalyst calcined at 500 ºC for two hours. Therefore, considering the previous results and the failure to detect CuO in the XRD tests, this peak at 280 ºC may be associated with highly dispersed Cu. On the other hand, Table 1 shows that the consumption of H_2 is lower than that necessary for reducing all the CuO present in the catalyst (ratio = 0.82), in agreement with previous studies [38].

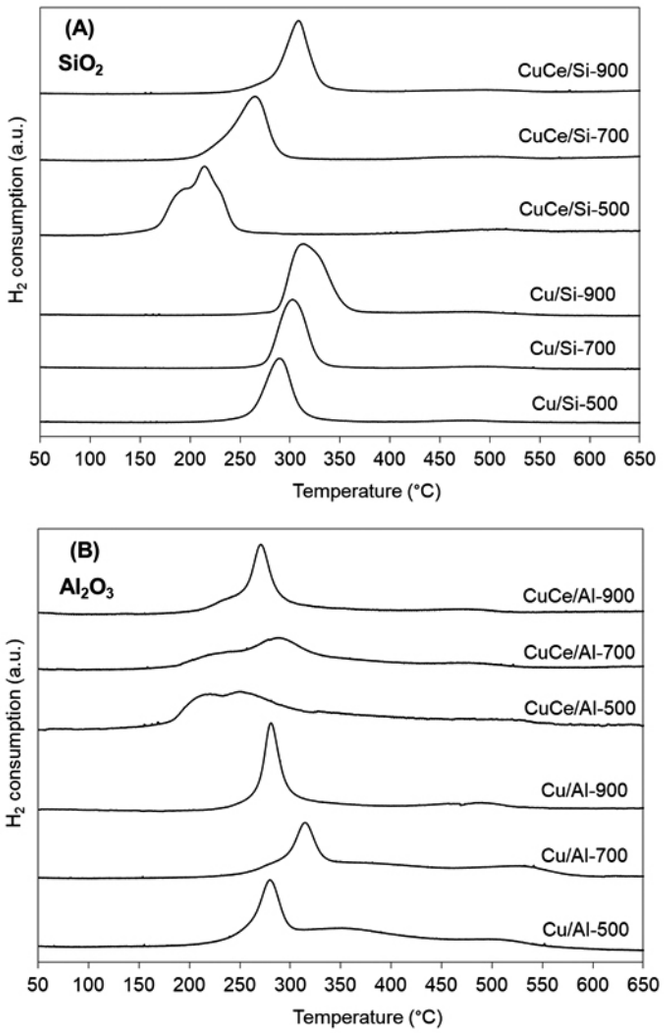

Figure 2: H_2-TPR curves of monometallic (Cu) and bimetallic (CuCe) catalysts calcined at 500 °C, 700 °C and 900 °C. (A) Supported on SiO_2; (B) Supported on Al_2O_3. Operation conditions: flow rate = 20 cm^3/min of 5%H_2 balance in He; heating rate = 10 °C/min; catalyst mass = 100 mg.

When the calcination temperature is increased to 700 ºC (Cu/Al-700), the reduction maximum is displaced to 315 °C, and H_2 consumption ratio decreases to 0.60, indicating that the Cu is harder to reduce than when calcining at 500 ºC. It is frequently found in the literature that increasing the calcination temperature leads to the displacement of the reduction peak to lower temperatures. In fact, Luo et al. [30] and Yahiro et al. [39] show that the reduction peaks are displaced to lower temperatures by calcining between 500 and 700 ºC. However, in these cases the high Cu load, 12% in the case of Luo et al. and 33% in the case of Yahiro et al., lead to the formation of CuO, so the displacement to lower temperatures is interpreted by these authors as an increased reduction ease of CuO due to a redispersion of this species. In our case no bulk CuO is formed, so the displacement of the reduction peak to higher temperature by calcining at 700 ºC must be explained by the formation of a Cu species that interacts to a greater degree with the alumina, hindering its reduction. Something similar was reported by Dumas et al. [40], who found that calcining a catalyst with 10% Cu at 600 to 750 ºC, a simultaneous displacement of the highly dispersed Cu peak from 242 ºC to 300 ºC took place, while the bulk CuO peak was displaced from 312 to 300 ºC, forming a single reduction peak with a maximum at 300 ºC. In other words, calcination at 700 ºC can generate the formation of less reducible species from highly dispersed Cu, at the same time generating more easily reducible species from bulk CuO.

Finally, when the calcination temperature is increased to 900 ºC (Cu/Al-900), the ease of reduction of Cu increases again, and the maximum is displaced to a lower temperature, very close to the one observed for the catalyst calcined at 500 ºC. In the literature it is reported that calcination at 900 ºC causes the formation of bulk $CuAl_2O_4$ [28], so this reduction peak may be associated with this species. However, the reduction maximum temperature observed with our catalyst is significantly lower than that reported in the literature for the bulk $CuAl_2O_4$ species. In fact, Severino et al. [38] report that the $CuAl_2O_4$ reduction peak is at 445 ºC, while Yahiro et al. [39] find the maximum at 410 ºC, and Sato et al. [41] report the reduction of Cu aluminate with a maximum at 450 ºC. On the other hand, and because of the low Cu load, our XRD analyses do not allow the formation of Cu aluminate to be discarded. Therefore, it is only possible to speculate that the peak at 280 ºC corresponds to the reduction of highly dispersed Cu species. Table 1 shows, however, that H_2 consumption (ratio = 0.59) is less than when calcining at 500 ºC, so the concentration of reducible Cu species decreases significantly by calcining between 500 and 900 ºC. The addition of CeO_2 produces important changes in the reduction curves with H_2 of the catalysts supported on alumina. The bimetallic catalyst calcined at 500 ºC shows two reduction peaks with reduction temperature maxima between 220 and 250 ºC attributed to Cu species of different sizes interacting with CeO_2, as discussed previously by our group [see ref. 25 and work cited therein]. The H_2 consumption with this catalyst, which is reported in Table 1, is also greater than in the monometallic catalyst calcined at the same temperature, confirming the formation of the Cu-CeO_2 interface. Increasing the calcination temperature to 700 ºC, the maximum of the first peak remains practically unshifted, but there is a shift of the second reduction peak's maximum from 250 to 290 ºC. However, the reduction maxima are lower than the maximum presented by the Cu monometallic catalyst calcined at 700 ºC, reflecting that the Cu-CeO_2 interaction has not disappeared completely in the catalyst calcined at 700 ºC. Calcining at 900 ºC results in a decrease of the area under the lower temperature peak, but it is clearly seen as a shoulder at 230 ºC. In a manner similar to what happens with the monometallic catalyst, the maximum of the higher temperature peak shifts to a reduction temperature lower than that found upon calcining at 700 ºC. The maximum is displaced from 290 to 270 ºC, a temperature 10 ºC lower than that found with the monometallic catalyst, suggesting that there still is an interaction with CeO_2. Table 1 shows that there is a slightly greater H_2 consumption than in the Cu monometallic catalyst calcined at the same temperature. Both observations lead to the conclusion that there still are sites corresponding to the Cu-CeO_2 interface in the catalyst calcined at 900 ºC.

The UV-vis DRS spectrum of the monometallic and bimetallic catalysts supported on SiO_2 is shown in Figure 3A. In the case of monometallic catalysts, the spectrum is dominated by a wide absorption band with a maximum at 660 nm. According to the literature, this band can be assigned to d-d transitions of Cu^{2+} in bulk CuO [42, 43]. In fact, Gang et al. [42] see this band clearly in unsupported CuO. The adsorption edge characteristic of bulk CuO particles is also clearly seen at wavelengths longer than 750-800 nm [44]. Therefore, the UV-vis DRS spectra are in perfect agreement with what is seen in the XRD and the TPR observations, which show the formation of bulk CuO in these catalysts regardless of the calcination temperature. On the other hand, the spectra of the bimetallic catalysts are dominated by the absorption band of cerium oxide. In fact, below 400 nm, the absorption band corresponding to Ce^{4+}-oxygen charge transfer transitions [45] is seen clearly, with a maximum close to 290 nm for the catalyst calcined at 500 ºC, which does not change significantly as the calcination temperature is increased. The zone above 400 nm is where the largest changes occur as the calcination temperature is increased. The band corresponding to CuO bulk species supported on SiO_2 becomes more intense as the calcination temperature is increased between 500 and 700 ºC, and it is clearly observable in the catalyst calcined at 900 ºC. Again, this result agrees with the phase separation between CuO and CeO_2, which was inferred from the XRD and TPR analyses.

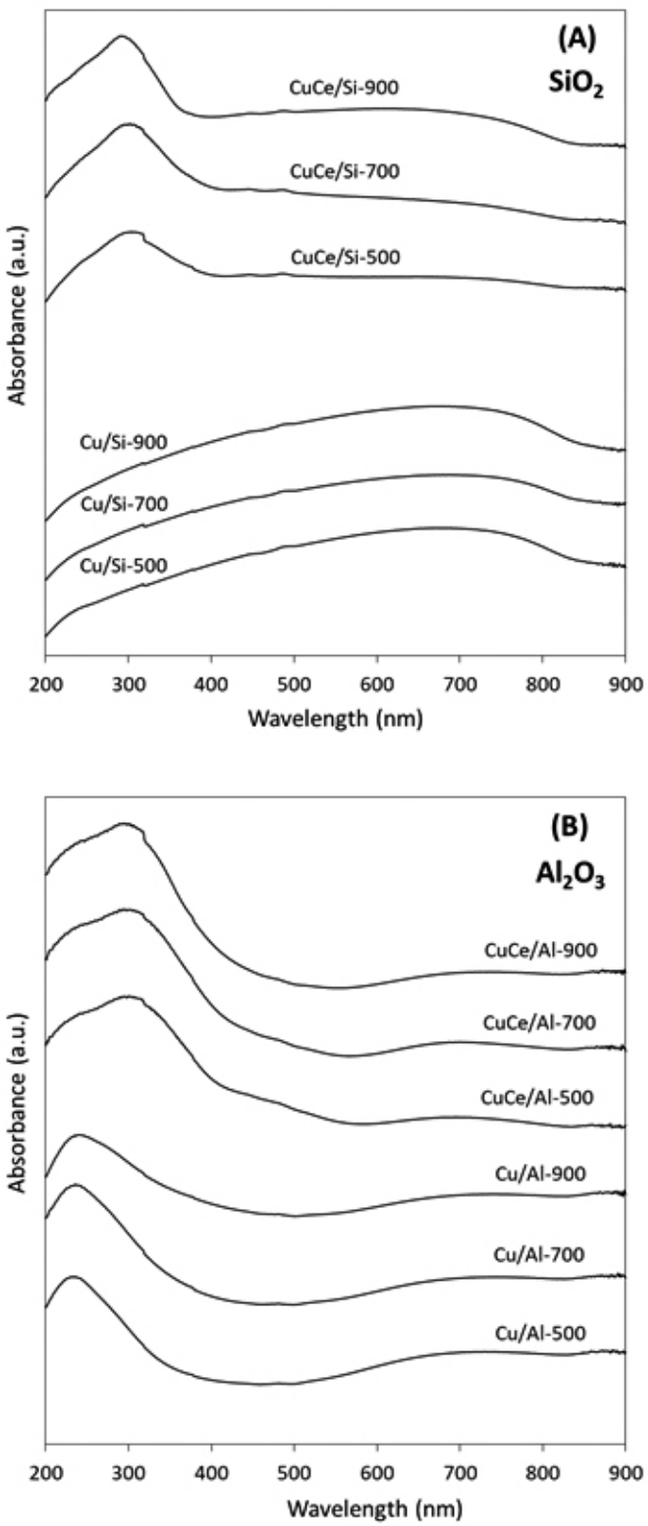

Figure 3: UV-vis DRS spectra of monometallic (Cu) and bimetallic (CuCe) catalysts calcined at 500 °C, 700 °C and 900 °C. (A) Supported on SiO_2; (B) Supported on Al_2O_3.

Figure 3B shows the UV-vis DRS spectra of the monometallic and bimetallic catalysts supported on alumina. The spectrum of the monometallic catalyst calcined at 500 ºC (Cu/Al-500) is very similar to those reported previously in the literature for the CuO/Al_2O_3 system [42, 46]. It is characterized by a band below 400 nm, with a maximum close to 240 nm that has been attributed to an $O^{2-} \rightarrow Cu^{2+}$ ligand-to-metal charge transfer [43], and a wide band with a maximum around 740 nm attributed to d-d transitions of Cu^{2+} with octahedral symmetry. It is important to point out that the adsorption edge characteristic of bulk CuO particles, clearly observable in the monometallic catalysts supported on SiO_2, is not seen in any of the catalysts supported on alumina. This is consistent with expectations, in view of the high dispersion of the Cu on this support observed by XRD. Calcining at a higher temperature does not result in major changes in the spectrum, except a widening of the band between 300 and 400 nm in the catalyst calcined at 900 ºC. This widening may be due to charge transfer involving Cu^{2+}-O^{2-} -Cu^{2+} species, or, possibly, cluster-like species [47]. In the spectrum of the bimetallic catalyst calcined at 500 ºC, a large peak is seen in the low wavelength zone, with a maximum at 300 nm and a shoulder at 240 nm. Considering what has been discussed previously, the former may be associated with Ce^{4+}-oxygen charge transfer transitions, and the latter to an $O^{2-} \rightarrow Cu^{2+}$ ligand-to-metal charge transfer. Between 600 and 850 nm, the characteristic band of the d-d transitions of Cu^{2+} are observed, and as in the case of the CuO/Al_2O_3 catalysts, it is not possible to see the adsorption edge characteristic of bulk CuO particles. Calcining at higher temperatures results in no important changes in the positions of the maxima of the absorption bands or signs of the adsorption edge of the bulk CuO particles. The above indicates that, in contrast with what was seen for the bimetallic catalysts supported on SiO_2, Cu retains a high dispersion even in the bimetallic catalyst calcined at 900 ºC. This result is in complete agreement with what was observed by XRD, where the CuO crystalline species is absent in the catalysts supported on alumina calcined between 500 and 900 ºC.

3.2 Catalytic activity

The conversion of CO as a function of reaction temperature for the monometallic Cu catalysts and the bimetallic Cu-Ce catalysts supported on SiO_2 is shown in Figure 4A. Except for the Cu monometallic catalyst calcined at 500 ºC, which presents a 7% conversion at 220 ºC, the monometallic catalysts calcined at 700 and 900 ºC are practically inactive in the temperature range used in this study. The XRD analysis, the TPR experiments, and the UV-vis DRS tests show that the Cu is found forming bulk CuO on the silica surface, a species that has low activity in the oxidation of CO [25, 38]. Adding CeO_2, the activity of the catalyst calcined at 500 ºC increases considerably, reaching almost 100% conversion at 120 ºC, as shown in Figure 4A. The great activity increase observed in the bimetallic catalyst confirms what has been reported extensively in the literature, that the sites of the Cu-CeO_2 interphase have a very high activity in this reaction [1-7]. In fact, the TPR experiments show that there is a strong interaction between the Cu and Ce species on the surface of this catalyst. As calcination temperature is increased to 700 °C, the activity drops considerably, in agreement with the decrease of the Cu-CeO_2 interactions, due mainly to the increase of the cerium oxide particle size reported in Table 1. It is interesting to note that in our previous paper [26], calcination at that same temperature of a Cu-Ce/SiO_2 catalyst of the same composition led to a total inactivation of the catalyst. The only difference with the present catalyst is that in the previous paper a silica with a larger surface area (Aerosil 200) was used, so the area of the support seems to play an important role in the stability of the Cu-CeO_2 interface. This will be considered in future studies. Calcination of the bimetallic catalyst at 900 °C leads to the total inactivation of the catalyst. The TPR experiments show clearly the separation of the CuO and CeO_2 phases in this catalyst, and the XRD results show that this phase separation is associated not only with the large growth of the CeO_2 particles on the surface of the silica, but also with the formation of the CuO bulk phase. The UV-vis DRS analysis of this catalyst confirms also the appearance of bulk CuO particles in the bimetallic catalyst calcined at 900 ºC.

Figure 4B shows the activity of catalysts supported on alumina. The activity of the monometallic Cu catalysts supported on alumina is low, but, in contrast with the catalysts supported on silica, the catalyst calcined at 900 °C shows some activity. The catalyst calcined at 900 ºC has an activity slightly higher than that of the catalyst calcined at 700 ºC. This result, which seems unexpected, is in agreement with the greater facility of reduction of the catalyst calcined at 900 ºC, compared to the one calcined at 700 °C, which was observed in the TPR experiments. This is a point that deserves more attention in future work. As expected, the addition of CeO_2 produces a strong increase of the activity of the catalysts. Obviously, the formation of interfacial Cu-CeO_2 sites on the surface of alumina explains this activity increase.

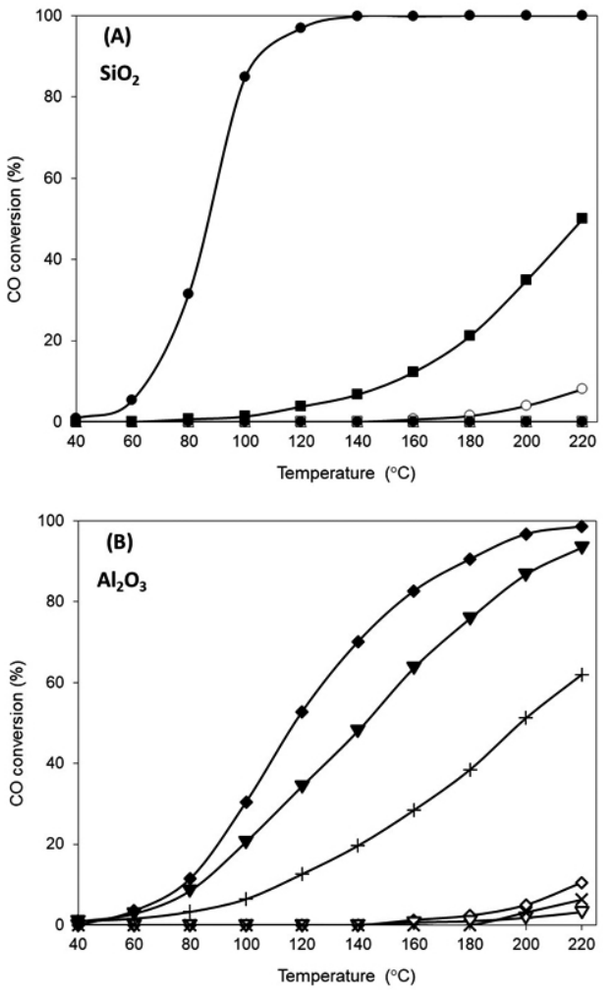

Figure 4: Activity in CO oxidation of monometallic (Cu) and bimetallic (CuCe) catalysts. (A) Supported on SiO_2: (o) Cu/Si-500; (□) Cu/Si-700; (Δ) Cu/Si-900; (•) CuCe/Si-500; (■) CuCe/Si-700; (▲) CuCe/Si-900; (B) Supported on Al_2O_3: (◊) Cu/Al-500; (▽) Cu/Al-700; (X) Cu/Al-900; (♦) CuCe/Al-500; (▼) CuCe/Al-700; (+) CuCe/Al-900.

What is most interesting, however, is that calcination at high temperatures, even though it decreases the activity of the bimetallic catalysts supported on Al_2O_3, it does so in a smaller proportion than when they are supported on silica. In effect, when calcining at 900 ºC, the CuCe/Si-900 catalyst is completely inactive, while the CuCe/Al-900 catalyst shows considerable activity in the oxidation of CO, achieving 60% conversion at 220 ºC. This greater activity must be associated with a greater stability of the Cu-CeO_2 interface on alumina than on silica. Indeed, the XRD experiments show that the CeO_2 particles are less sintered on alumina than on silica, increasing in a somewhat pronounced way their size, as reported in Table 1. At the same time, the XRD and UV-vis DRS analyses do not detect the appearance of bulk CuO on alumina, indicating that the sintering of Cu to form bulk CuO is also less on alumina than on silica. Clearly, the inert character of silica favors the sintering of the Cu species and CeO_2 particles and their segregation on the surface of the silica as the temperature is increased, decreasing strongly the concentration of sites on the interface. Supporting on alumina, the interaction with the support inhibits the growth and separation of the Cu species and CeO_2 particles, allowing interfacial Cu-CeO_2 sites even after calcining at 900 ºC.

The results of the activity of the different monometallic and bimetallic catalysts supported on SiO_2 and Al_2O_3 in the decomposition of N_2O are shown in Figures 5A and 5B, respectively.

Figure 5A shows all the monometallic Cu catalysts supported on silica are inactive in the decomposition of N_2O. As expected, the addition of CeO_2 improves noticeably the activity of the catalysts, achieving more than 80% conversion with the catalyst calcined at 500 ºC. This result shows clearly that the Cu-CeO_2 interface is responsible for the catalytic activity of these systems, as already reported in the literature [13-16]. If the Cu-CeO_2 interface is responsible for the catalyst's activity, it would be expected that the N_2O decomposition activity should follow the same trend as the oxidation activity of CO with O_2. In effect, this is what happens. With calcining at 700 ºC, the activity decreases substantially, and it is practically nil after calcining at 900 ºC, following the same trend as in the CO oxidation reaction. The decrease of the interfacial sites due to the sintering and segregation of Cu species and CeO_2 particles on the surface of the silica account for the behavior in the decomposition of N_2O.

When alumina is used for support, the behavior of the monometallic Cu catalysts is very different from that observed on Cu supported on silica. Figure 5B shows that the monometallic Cu catalysts have a noticeable catalytic activity in the decomposition of N_2O, which is consistent with other studies [36, 48], achieving 63.5% conversion at 600 ºC in the case of the catalyst calcined at 500 ºC. Increasing the calcination temperature to 700 ºC, reduces the activity at 600 ºC to 48.1%, and calcining at 900 ºC increases it slightly, reaching 51.8% conversion. This behavior coincides with what is seen in the TPR experiments, where the ease of reduction increases by calcining between 700 and 900 ºC. On the other hand, the addition of CeO_2 produces an increase in the activity of all the catalysts supported on alumina. This activity increase, due to adding CeO_2, is not as important as that observed when using SiO_2 for support, due to the activity of the monometallic Cu catalysts supported on alumina. The bimetallic catalyst calcined at 500 ºC achieves 95.4% conversion at 600 ºC, which is significantly greater than the 63.5 % achieved by the monometallic catalyst.

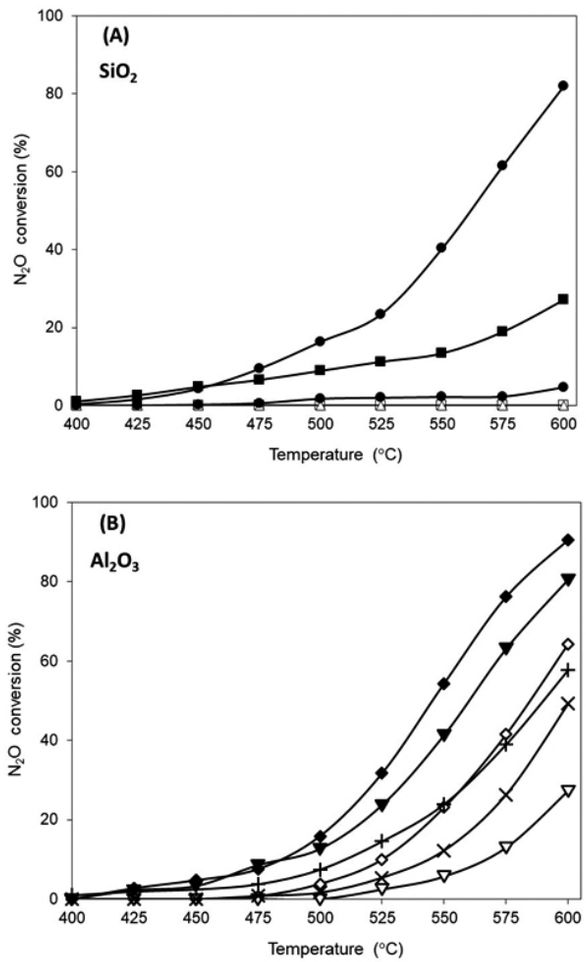

Figure 5: Activity in N_2O decomposition of monometallic (Cu) and bimetallic (CuCe) catalysts. (A) Supported on SiO_2: (o) Cu/Si-500; (□) Cu/Si-700; (Δ) Cu/Si-900; (•) CuCe/Si-500; (■) CuCe/Si-700; (▲) CuCe/Si-900; (B) Supported on Al_2O_3: (◊) Cu/Al-500; (▽) Cu/Al-700; (X) Cu/Al-900; (♦) CuCe/Al-500; (▼) CuCe/Al-700; (+) CuCe/Al-900.

When the bimetallic Cu-Ce catalyst supported on alumina is calcined at 700 ºC (Figure 5B), the activity at 600 ºC drops slightly to 86.5%. This is significantly higher than the 48.1% conversion activity of the monometallic catalyst calcined at the same temperature, demonstrating the importance of the activity of the Cu-CeO_2 interface. Increasing calcination temperature at 900 °C, the activity of the bimetallic Cu-Ce catalyst drops to 61.1%, and the difference with respect to the conversion of the monometallic Cu catalyst (48.1%) decreases. It is evident that calcination at 900 °C causes a decrease of the concentration of interfacial sites, but their concentration is still sufficiently high to keep an activity greater than that of the monometallic catalyst calcined at the same temperature.

In short, the results of the N_2O decomposition activity confirm that the sites of the Cu-CeO_2 interface are highly active in this reaction and that the stability of this interface is better when it is supported on alumina rather than on silica. Therefore, the characterization of the catalysts as well as their activity in the oxidation of CO with O_2 and the decomposition of N_2O reactions show that the thermal stability of the Cu-CeO_2 interface is better when using alumina for support, in the calcination temperature range of 500 ºC to 900 ºC used in the present study.

4.- CONCLUSIONS

The results clearly show that the support has an important influence on the formation and stability of the Cu-CeO_2 interface. Although the formation of interfacial Cu-CeO_2 sites is favored in the catalysts calcined at 500 ºC using silica for support, the thermal stability of the interface is low. Calcination at 900 ºC causes the growth of the Cu species and CeO_2 particles, and their complete separation on the surface of the silica. The disappearance of the Cu-CeO_2 interfacial sites is responsible for the catalytic activity in the oxidation of CO and the decomposition of N_2O. On the one hand, the inert character of silica improves the interaction between Cu and CeO_2, but on the other hand, it favors the sintering of these species as the calcination temperature is increased.

In contrast, if Al_2O_3 is used for support, the bimetallic catalysts maintain an important activity in both reactions when they are calcined at 900 ºC, due to a greater stability of the Cu-CeO_2 interface. This stability is attributed to the fact that the interaction of the Cu and Ce species with the support decreases the sintering of the Cu and CeO_2 particles, such that even after calcining at 900 ºC, some interfacial Cu-CeO_2 sites still exist on the surface of the alumina, generating an important catalytic activity in both reactions.

ACKNOWLEDGEMENTS

The authors acknowledge gratefully the financial support of this work under Fondecyt project 1161227.

REFERENCES

1. Liu W, Flytzani-Stephanopoulos M (1995) J. Catal. 153: 304-316
2. Kundakovic L, M. Flytzani-Stephanopoulos M (1998) J. Catalysis 179: 203-221
3. Li Y, Fu Q, Flytzani-Stephanopoulos M (2000) Applied Catalysis B 27: 179-191
4. Kundakovic L, Flytzani-Stephanopoulos M (1998) Applied Catalysis A 171: 13-29
5. Liu Y, Fu Q, Flytzani-Stephanopoulos M (2004) Catalysis Today 93: 241-246
6. Madier Y, Descorme C, Le Govic A, Duprez D (1999) J. Phys. Chem. B 103: 10999-11006
7. Martinez-Arias A, Fernandez-Garcia M, Galvez O, Coronado J, Anderson J, Conesa J, Soria J, Munuera, G (2000) J. Catal. 195: 207-216
8. Yao S, Mudiyanselage K, Xu W, Johnston-Peck A, Hanson J, Wu T, Stacchiola D, Rodriguez J, Zhao H, Beyer K, Chapman K, Chupas P, Martinez-Arias A, Si R, Bolin T, Liu W, Senanayake S (2014) ACS Catalysis 4: 1650-1661
9. Wang W, Du P, Zou S, He H, Wang R, Jin Z, Shi S, Huang Y, Si R, Song Q, Jia C, Yan C (2015) ACS Catalysis 5: 2088-2099
10. Davo-Quiñonero, Navlani-Garcia M, Lozano-Castello D, Bueno-Lopez A, Anderson J (2016) ACS Catalysis 6: 1723-1731
11. Benedetto A, Landi G, Lisi L (2017) International Journal of Hydrogen Energy 42: 12262-12275
12. Wang X, Rodriguez J, Hanson J, Gamarra D, Martinez-Arias A, Fernandez-Garcia M (2006) J. Phys. Chem. B 110: 428-434
13. Adamski A, Zajac W, Zasada F, Sojka Z (2012) Catalysis Today 191: 129-133
14. Zhou H, Huang Z, Sun C, Qin F, Xiong D, Shen W, Xu H (2012) Applied Catalysis B 125: 492-498
15. Zabilskiy M, Erjavec B, Djinovic P, Pintar A (2014) Chemical Engineering Journal 254: 153-162
16. Zabilskiy M, Djinovic P, Erjavec B, Drazic G, Pintar A (2015) Applied Catalysis B 163: 113-122
17. Hevia M, Pérez-Ramírez J (2008) Applied Catalysis B 77: 248-254
18. Gunawardana P, Lee H, Kim D (2009) International Journal of Hydrogen Energy 34: 1336-1341
19. Djinovic P, Levec J, Pintar A (2008) Catalysis Today 138: 222-227
20. Pintar A, Batista J, Hocevar S (2007) Journal of Colloid and Interface Science 307: 145-157
21. Djinovic P, Batista J, Pintar A (2008) Applied Catalysis A 347: 23-33
22. Pradhan S, Reddy A, Devi R, Chilkuri S (2009) Catalysis Today 141: 72-76
23. Sun Y, Hla S, Duffy G, Cousins A, French D, Morphet L, Edwards J, Roberts D (2010) Catalysis Communications 12: 304-309
24. Schwarz J, Contescu C, Contescu A, Chem. Rev. (1995) 95: 477-510
25. Aguila G, Gracia F, Araya P (2008) Applied Catalysis A 343: 16-24
26. Aguila G, Guerrero S, Araya P (2013) Applied Catalysis A 462: 56-63
27. Friedman R, Freeman J, Lytle W (1978) Journal of Catalysis 55: 10-28
28. Strohmeier B, Leyden D, Field R, Hercules D (1985) Journal of Catalysis 94: 514-530
29. Cheektamarla P, Epling W, Lane A (2005) Journal of Power Sources 147: 178-183
30. Luo M, Fang P, He M, Xie Y (2005) Journal of Molecular Catalysis A: Chemical 239: 243-248
31. Liu Z, Amiridis A, Chen Y (2005) J. Phys. Chem. B 109: 1251-1255
32. Zhou R, Jiang X, Mao J, Zheng X (1997) Applied Catalysis A 162: 213-222
33. Ma Z, Yang C, Wei W, Li W, Sun Y (2005) J. Mol. Catal. A: Chem. 231: 75-81
34. Shan W, Shen W, Li C, (2003) Chem. Mater. 15: 4761-4767
35. Dow W, Wang Y, Huang T (1996) Journal of Catalysis 160: 155-170
36. Yao K, Jaenicke S, Lin J, Tan K (1998) Applied Catalysis B 16: 291-301
37. Xiaoyuan J, Liping L, Yingxu C, Xiaoming Z (2003) Journal of Molecular Catalysis A 197: 193-205
38. Severino F, Brito J, Carias O, Laine J (1986) Journal of Catalysis 102: 172-179
39. Yahiro H, Nakaya K, Yamamoto T, Saiki K, Yamaura H (2006) Catalysis Communications 7: 228-231
40. Dumas J, Geron C, Kribii A, Barbier J (1989) Applied Catalysis 47: L9-L15
41. Sato S, Iijima M, Nakyama T, Sodesawa T, Nozaki F (1997) Journal of Catalysis 169: 447-454
42. Gang L, Grondelle J, Anderson B, van Santen R (1999) Journal of Catalysis 186: 100-109
43. Praliaud H, Mikhailenko S, Chajar Z, Primet M (1998) Applied Catalysis B 16: 359-374
44. Shimokawabe M, Takesawa N, Kobayashi H (1982) Applied Catalysis 2: 379-387
45. Martinez-Arias A, Fernandez-Garcia M, Salamanca L, Valenzuela R, Conesa J, Soria J (2000) J. Phys. Chem. B 104: 4038-4046
46. Hu H, Dong L, Shen M, Liu D, Wang J, Ding W, Chen Y (2001) Applied Catalysis B 31: 61-69
47. S. Velu S, K. Susuki, K M. Okazaki M, M. Kapoor M, T. Osaki T, F. Ohashi F (2000) Journal of Catalysis 194: 373-384
48. Dandekar A, Vannice M (1999) Applied Catalysis B 22: 179-200